Triangular lattice of carbon nanotube arrays for negative index of refraction and subwavelength lensing effect

Y. Wang, X. Wang, J. Rybczynski, D. Z. Wang, K. Kempa, and Z. F. Ren[a)]
Department of Physics, Boston College, Chestnut Hill, Massachusetts 02467

(Received 2 June 2004; accepted 31 January 2005; published online 8 April 2005)

Self-assembly of polystyrene microspheres has been utilized in a two-step masking technique to prepare triangular lattices of catalytic nanodots at low cost. Subsequent triangular lattices of aligned carbon nanotubes on a silicon substrate are achieved by plasma-enhanced chemical vapor deposition. Nickel is used both in the nanodots and in the secondary mask. The triangular lattices of carbon nanotube arrays as two-dimensional photonic crystals show higher geometrical symmetry than the hexagonal lattices previously reported, enabling broader applications including negative index of refraction and subwavelength lensing effect. © *2005 American Institute of Physics*. [DOI: 10.1063/1.1900941]

Since the discovery of carbon nanotubes,[1] tremendous progress has been made, not only in controlling the growth yields and atomic structures of carbon nanotubes,[2–5] but also in aligning their orientations,[6–9] varying site densities,[10] etc., for various potential applications. Driven by the very recent accelerating development of nanoscale devices,[11–14] most of which utilize carbon nanotubes not in a large quantity at a time but one by one, and the importance to efficiently integrate these devices as functional units at high density, more specific preparation techniques dealing with individual nanotubes over a relatively large area are seriously demanded. One of the most important research areas is to make ordered configurations in which single nanotubes can be grown at selective locations on substrates without using expensive patterning techniques, such as electron-beam lithography or any elaborate microscopic maneuvers. Self-assembly of polystyrene microspheres[15] was utilized by Kempa *et al.*[16] and perfected soon after[17] to pattern hexagonal nickel (Ni) dots and subsequently grow aligned carbon nanotube arrays in large-scale hexagonal lattices at low cost. Those arrays have been used as photonic crystals and many other applications due to the periodic structures composed of single carbon nanotubes with three-fold symmetry. However, other geometries with higher degrees of ordering and symmetry will be even more useful if they can be produced inexpensively. This letter presents a low-cost technique to prepare triangular lattices of aligned carbon nanotube arrays by further exploring the self-assembly of polystyrene microspheres, and the potential applications of these arrays in negative index of refraction and subwavelength lensing effect.

The challenge to arrange individual carbon nanotubes in a certain periodicity is to form the catalytic dots at periodic locations. This is again accomplished herein by forming the periodic structure from self-assembled polystyrene microspheres to avoid the costly lithographic methods. It was found out that in order to have only a single nanotube with uniform morphology grown from each catalytic dot (single growth), the catalyst must have a moderate volume and a proper shape. In order to form triangular lattices, a second-order masking procedure, one step further from the previous single-layer masking technique in the fabrication of hexagonal lattice structures, is adopted.

Figure 1 shows the scheme of fabricating a triangular lattice pattern of catalyst dots on a silicon (Si) substrate from which individual aligned carbon nanotubes are grown. A thin layer of photoresist (MicroPosit S1818) is first spin coated onto a Si substrate (~0.5 mm thick), and a monolayer of polystyrene microspheres (980 nm in diameter is reported here, but other diameters were often used in experiments) self-assembled on an aqueous surface[15] is then transferred onto the photoresist layer. The photoresist thickness is 1–2 μm at a spin rate of 4000 rpm. The assembly is then

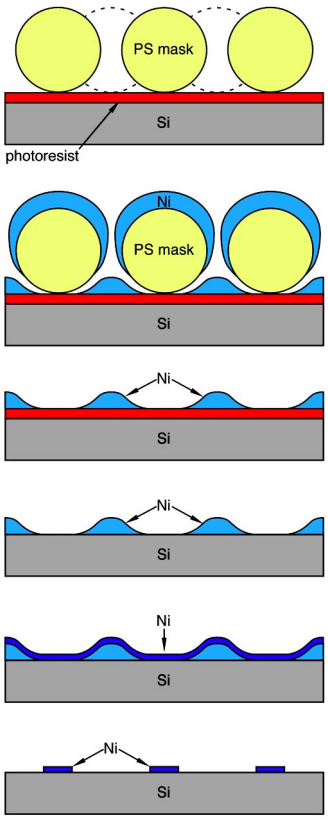

FIG. 1. (Color online) Step-by-step schematics of a two-step masking technique using microsphere self-assembly. Note in the top two graphs, the cross section is taken not to pass the sphere centers.

[a)]Author to whom correspondence should be addressed; electronic mail: renzh@bc.edu

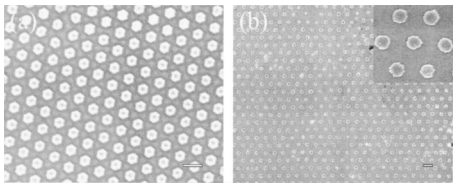

FIG. 2. SEM characterization for Steps 3 and 6. (a) Continuous Ni network on the photoresist layer after removing the spheres. The open hexagonal dots are the underlying photoresist exposed by the holes of the Ni network. The shade in each dot is due to charge accumulation. (b) Triangular lattice of patterned Ni dots on Si substrate. Inset: High magnification view of the round-shaped Ni dots. Scale bars: 1 μm.

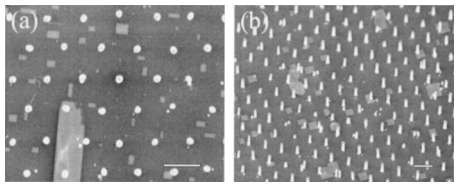

FIG. 3. SEM images of triangular lattice of as-grown aligned carbon nanotube arrays on Si substrate. (a) Top view at high magnification showing the almost perfect periodicity and alignment. (b) Side view at low magnification over a large area. The random rectangles on the background are from the original Si substrate, which has nothing to do with the procedures adopted. Note Fig. 2(b) and Fig. 3 are taken from different samples. Scale bars: 1 μm.

loaded into an rf magnetron sputtering system and a Ni layer as thick as 200 nm is sputtered through the sphere apertures, forming two continuous networks: One on the spheres and the other on the photoresist layer. The formation of the continuous network is because of the fact that sputtering deposits Ni onto all of the exposed surfaces. Next, the spheres are completely removed by ultrasonication in water, leaving holes [open hexagonal dots in Fig. 2(a)] at the original positions of the spheres. Then, the sample is slowly immersed into 99.9% tetrahydrofuran to dissolve the underlying photoresist. A strong permanent magnet (NdFeB, Grade N50, not shown in Fig. 1) is put right under the substrate which constantly attracts the Ni network toward the substrate during the dissolving process to prevent sliding and folding of the Ni network due to minor disturbances. The dissolving procedure is repeated for a complete removal of the polystyrene material with no significant damage observed to a Ni network of 1 cm^2. When the sample is dried, the magnet can be removed while the Ni network stays on the Si surface due to Van de Waal's force. This network is used as a secondary mask for a Ni evaporation (60 nm). The directly evaporated Ni through the holes is much more firmly adhered to the Si surface than the thickened Ni network that can be detached mechanically by another ultrasonication (40 kHz) in water. It happens in such a manner that the Ni layer close to the hole edge breaks up during ultrasonication, leaving isolated Ni dots on the Si substrate. Figure 2(b) shows the scanning electron microscopy (SEM) image of the resulting Ni dots with uniform shape in a triangular lattice pattern, with the high magnification image shown in the inset. It is worth noting that the Ni layer does not seem to break up exactly at the edge of the holes, but somewhere inside of the holes, which is illustrated by the fact that the size of the Ni dots (400–450 nm in diameter) generally appears to be smaller than the original hole size (650–700 nm in diameter). This can possibly be explained by either the inability to accurately define the hole edge by SEM images where very little material is present or that the evaporated Ni becomes looser due to the height difference around the edge area. The process is fairly repeatable. The area with good periodicity is about a few submillimeters square, which can be scaled up to a few square millimeters with care at each step.

The periodic Ni dots are then used as catalysts to grow aligned carbon nanotubes by plasma-enhanced chemical vapor deposition. The growth is carried out for 10 min at 550 °C, using a 0.4 A plasma current and 1 min pregrowth plasma etching.[17] C_2H_2 and NH_3 are used as reaction gases at a ratio of 1:2, while the system pressure is kept within 5–10 Torr during growth. Triangular lattice arrays of aligned carbon nanotubes of diameters about 200–300 nm are therefore obtained and characterized by top and inclined views respectively, as shown in Figs. 3(a) and 3(b). At most of the periodic spots, only single nanotubes are grown with excellent alignment, but some double growth also occurs at a few spots due to the irregular shape of some catalysts. The irregularity could be caused by the defects in the original monolayer of polystyrene microspheres, nonuniform thickness of the sputtered Ni layers, leftover photoresist scum, and excessive plasma etching. Better qualities can be expected by improving the handling in each patterning step and optimizing the growth parameters. Nevertheless, the idea is clearly demonstrated. The well-defined round shape of the catalyst dots are more suitable to yield single growth compared to the quasi-triangular shape of catalyst islands before. The fabrication technique can also be applied to obtain triangular lattice arrays of aligned nanowires, such as ZnO, etc.

One of the potential applications of the periodic nanotube arrays is that they can act as two-dimensional photonic crystals. Compared to our previous honeycomb arrays of carbon nanotubes, this triangular photonic crystal has higher rotational symmetry and planar uniformity (each nanotube is two dimensionally equivalent in position), which enables more applications, such as negative index of refraction and subwavelength lensing effects.[18,19] Here, we present the calculated photonic band structure of these triangular arrays of nanotubes for transverse magnetic modes (electric field parallel to the nanotubes), as shown in Fig. 4(a), where the lattice constant $a=1$ μm, the nanotube diameter $D=0.3$ μm, and the nanotubes (multiwalled and bamboolike) are treated as perfect metallic rods at optical frequencies.[20] There is an absolute band gap below the first band due to the metallic properties of the nanotubes. A frequency range exists around 2.76×10^{14} Hz ($a/\lambda=0.92$), where the band is almost isotropic. The equifrequency contours, centered at the Γ point, are essentially circular in that region, and their radii decrease with increasing frequency. Therefore, an effective isotropic negative refractive index can be defined, which is $n_{\text{eff}}=-1$ for 2.76×10^{14} Hz, meaning negative refraction could occur in a simple slab of the triangular arrays of carbon nanotubes. To demonstrate the subwavelength lensing effect, one needs to work at the frequency range where $a/\lambda\leqslant0.5$ (Ref. 21) to avoid high reflection at the slab surface. This can be easily achieved by filling the internanotube space with dielectric materials, so that all the bands move downward without changing their pattern. For example, if we choose the dielectric material with $\varepsilon=12$ (i.e., Si at 1.55 μm wavelength), the negative index $n_{\text{eff}}=-1$ then occurs at 0.75×10^{14} Hz ($a/\lambda=0.25$). Figure 4(b) demonstrates the simulated subwavelength lensing effect. More importantly, the fabrication tech-

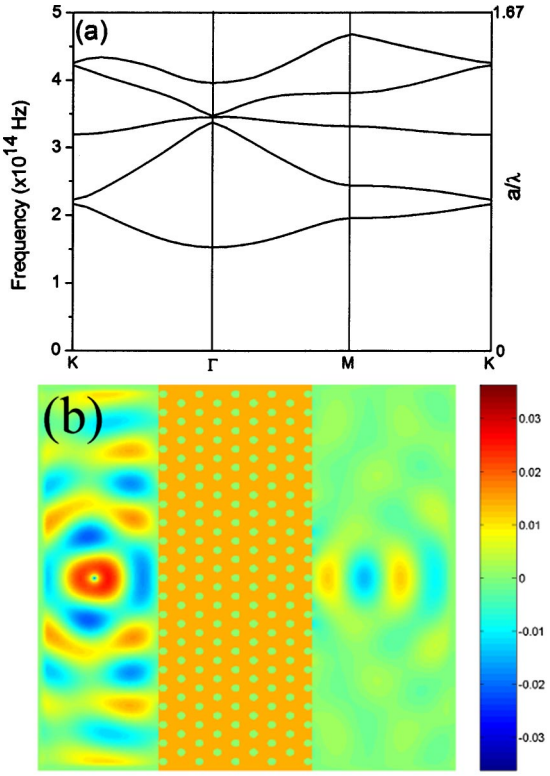

FIG. 4. (Color online) Negative index of refraction and subwavelength lensing effect. (a) Band diagram (transverse magnetic mode) of a triangular lattice of carbon nanotube arrays calculated by the plane wave expansion method. (b) Subwavelength lensing effect of a slab of triangular lattice of carbon nanotube arrays (nine layers) in dielectric matrix ($\varepsilon=12$). Here, we show a simulated snapshot of the electric-field intensities produced by a point source of frequency 0.75×10^{14} Hz placed on the left side of the slab at a distance of 4 μm using the finite-different time-domain method. There is a point image on the right side of the slab. The transverse size of the image is $\Delta=0.86\lambda$ (resolution $R=\Delta/2$), which is clearly subwavelength. The color gradient bar quantifies the relative electric-field intensity.

nique has the flexibility to increase the volume of individual catalytic nanodots by increasing the evaporation thickness of Ni or reducing pregrowth plasma etching, both of which would result in larger nanotube diameters and larger filling factor to further open the photonic band gap drastically. And, by adopting polystyrene microspheres of different diameters, both effects can be demonstrated in different frequency ranges.

In conclusion, triangular lattices of Ni dots are prepared inexpensively by a two-step masking approach based on self-assembly of polystyrene microspheres. Periodic arrays of aligned carbon nanotubes are also grown by plasma-enhanced chemical vapor deposition. The proposed patterning technique produces catalytic Ni dots in a suitable shape for the single growth of carbon nanotubes. The geometry—composed of isolated carbon nanotubes—is shown to be suitable for broader application purposes including negative index of refraction and subwavelength lensing effect. The patterning technique can be generally applied to fabricate triangular lattice arrays of other materials.

The work was supported by the U.S. Army Research Development and Engineering Command, Natick Soldier Center, under Grant No. DAAD16-03-C-0052 for four of the authors (Y. W., J. R., K. K., and Z. F. R.), and by NSF NIRT under Grant No. 0304506 for two of the authors (Y. W. and Z. F. R.).

[1] S. Ijima, Nature (London) **354**, 56 (1991).
[2] Z. J. Shi, X. H. Zhou, Z. X. Jin, Z. N. Gu, J. Wang, S. Q. Feng, X. L. Xu, and Z. Q. Liu, Solid State Commun. **97**, 371 (1996).
[3] X. S. Li, H. W. Zhu, B. Jiang, J. Ding, C. L. Xu, and D. H. Wu, Carbon **41**, 1664 (2003).
[4] J. M. Zuo, I. Vartanyants, M. Gao, R. Zhang, and L. A. Nagahara, Science **30**, 1419 (2003).
[5] H. T. Cui, X. J. Yang, M. L. Simpson, D. H. Lowndes, and M. Varela, Appl. Phys. Lett. **84**, 4077 (2004).
[6] Z. F. Ren, Z. P. Huang, J. W. Xu, J. H. Wang, P. Bush, M. P. Siegal, and P. N. Provencio, Science **282**, 1105 (1998).
[7] K. B. K. Teo, M. Chhowalla, G. A. J. Amaratunga, W. I. Milne, D. G. Hasko, G. Pirio, P. Legagnenx, F. Wyczisk, and D. Pribat, Appl. Phys. Lett. **79**, 1534 (2001).
[8] L. Delzeit, C. V. Nguyen, R. M. Stevens, J. Han, and M. Meyyappun, Nanotechnology **13**, 280 (2002).
[9] Z. W. Pan, H. G. Zhu, Z. T. Zhang, H. J. Im, S. Dai, D. B. Beach, and D. H. Lowndes, J. Phys. Chem. B **107**, 1338 (2003).
[10] Y. Tu, Z. P. Huang, D. Z. Wang, J. G. Wen, and Z. F. Ren, Appl. Phys. Lett. **80**, 4018 (2002).
[11] R. H. Baughman, C. Cui, A. A. Zakhidov, Z. Iqbal, J. N. Barisci, G. M. Spinks, G. G. Wallace, A. Mazzoldi, D. D. Rossi, A. G. Rinzler, O. Jaschinski, S. Roth, and M. Kertesz, Science **284**, 1340 (1999).
[12] A. Bachtold, P. Hadley, T. Nakanishi, and C. Dekker, Science **294**, 1317 (2001).
[13] K. Keren, R. S. Berman, E. Buchstab, U. Sivan, and E. Braun, Science **302**, 1380 (2003).
[14] A. Modi, N. Koratkar, E. Lass, B. Wei, and P. W. Ajayan, Nature (London) **424**, 171 (2003).
[15] J. Rybczynski, U. Ebels, and M. Giersig, Colloids Surf., A **219**, 1 (2003).
[16] K. Kempa, B. Kimball, J. Rybczynski, Z. P. Huang, P. F. Wu, D. Steeves, M. Sennett, M. Giersig, D. V. G. L. N. Rao, D. L. Carnahan, D. Z. Wang, J. Y. Lao, W. Z. Li, and Z. F. Ren, Nano Lett. **3**, 13 (2003).
[17] Y. Wang, J. Rybczynski, D. Z. Wang, W. Z. Li, B. Kimball, K. Kempa, and Z. F. Ren, Appl. Phys. Lett. **85**, 4741 (2004).
[18] M. Notomi, Phys. Rev. B **62**, 10696 (2000).
[19] X. Wang and K. Kempa, cond-mat/0410560.
[20] Y. Wang, K. Kempa, B. Kimball, J. B. Carlson, G. Benham, W. Z. Li, T. Kempa, J. Rybczynski, A. Herczynski, and Z. F. Ren, Appl. Phys. Lett. **85**, 2607 (2004).
[21] C. Luo, S. G. Johnson, and J. D. Joannopoulos, Phys. Rev. B **65**, 201104 (2002).